J. Fluid Mech. (1988), vol. 189, pp. 117–134
Printed in Great Britain

The long-wave instability of a defect in a uniform parallel shear

By J. LERNER AND E. KNOBLOCH
Department of Physics, University of California, Berkeley, CA 94720, USA

(Received 28 October 1986 and in revised form 28 August 1987)

The stability properties of an inviscid, parallel, incompressible, free shear flow are studied. The shear profile is that of an unbounded, plane Couette flow containing a defect, or transition zone, whose magnitude ϵ is assumed to be small. The linearized eigenvalue problem is solved first for discretized models. When the defect has a finite thickness, the instability is confined to longitudinal wavenumbers, $k \leqslant O(\epsilon)$, in contrast to the more common $O(1)$ bandwidth, in units of inverse shear length. This observation motivates the application of a long-wave expansion to a smooth defect profile. A double expansion in both k and ϵ captures the whole waveband of the instability, and yields convergent expansions for the unstable eigenfunctions and for the dispersion relation describing their growth rate. The fastest growing modes are determined, and their back-reaction on the basic shear is calculated.

1. Introduction and formulation of the problem

The stability or instability of shear flows is a subject of major importance in geophysics and astrophysics, and occupies a central place in the studies of hydrodynamic stability (Drazin & Reid, 1981). Analytic investigation is often complicated by the absence of stability boundaries and the tendency of many shear flows to be subscritically unstable, i.e. to be unstable with respect to finite amplitude perturbations for parameter values for which linear theory predicts stability. In addition, shear-flow problems are generally devoid of naturally appearing small parameters, although these can be introduced by restricting the analysis to large longitudinal wavelengths, i.e. small wavenumbers, k. Such long-wave expansions, hereinafter LWE, have led to a number of useful results (Drazin & Howard, 1962; Tatsumi, Gotoh & Ayukawa 1964), but are difficult to apply to the usually dominant instability on the scales of the shear itself.

The above considerations suggest the study of a problem containing a small parameter in which the dominant instability occurs only at the long wavelengths. The choice of problem, suggested to us by J.-P. Zahn, is motivated by the likelihood that unbounded, plane Couette flow is unstable with respect to finite-amplitude perturbations that introduce inflexion points into the flow. We call such a perturbation a defect. The resulting flow, Couette flow, together with the defect, satisfies the necessary conditions for instability. Of interest is the effect of the Couette flow on the instability generated by the defect. To formulate the problem, we assume that the defect is maintained, and study the linear stability of the combined shear flow. The presence of the defect introduces the required small parameter into the problem.

The problems we study are all inviscid, two-dimensional, incompressible, plane-parallel shear flows with velocity of the form $\boldsymbol{u} = (u_0(y;\ \epsilon), 0)$, where ϵ indicates the dimensionless amplitude of the defect and (x, y) are coordinates parallel and transverse to the flow. If we write the stream function for a perturbation of the flow in the form $\Psi = \mathrm{Re}\{\phi(y) \exp[\mathrm{i}k(x-ct)]\}$ then the function $\phi(y)$ satisfies the Rayleigh equation

$$\left[(u_0(y;\epsilon)-c)\left(\frac{\mathrm{d}^2}{\mathrm{d}y^2}-k^2\right)-u_0''(y;\epsilon)\right]\phi(y) = 0, \tag{1.1a}$$

where k is the wavenumber of the disturbance in the flow direction, and c is its phase speed. Throughout the paper we restrict ourselves to temporal instability, and therefore take k to be real. Since (1.1a) depends on k^2, we may in fact assume $k > 0$. Consequently, our results are more applicable to free shear flows than to mixing layers. As boundary conditions, we impose

$$\phi(\pm\infty) = 0, \tag{1.1b}$$

corresponding to an unbounded flow. Equations (1.1) constitute an eigenvalue problem for the, possibly complex, phase speed $c(k,\epsilon)$. A problem of this type was first considered by Gill (1965; see also Huerre 1983), who showed quite generally that finite boundaries serve to create an amplitude threshold for instability. This is the main reason for imposing boundary conditions at infinity. The existence of such a threshold could explain the apparent absence of two-dimensional, finite amplitude instabilities of bounded plane Couette flow noted by Orszag & Kells (1980). Their numerical simulations of three-dimensional plane Couette flow do, however, show a transition to turbulence even in the absence of linear instability. This appears to be caused by three-dimensional inflexion points transverse to the flow, produced by the evolution of large-amplitude initial conditions. Thus, whether imposed by hand as above, or induced nonlinearly, inflexional corrections to the basic shear appear to govern the transition to turbulence.

Of the three shear flows studied in this paper, the first two are discrete, exactly solvable, and serve to motivate the analysis of the smooth profile. The analysis of the discrete models is provided in §2, and shows that the bandwidth of the instability is reduced by the mean shear to $O(\epsilon)$ near $k = 0$. The maximum growth rate of the instability remains, however, of $O(\epsilon)$, its magnitude in the absence of the mean shear. These results suggest that a double expansion, in both k and ϵ, may be able to capture the entire band of unstable wavenumbers, and, in particular, the fastest growing modes. Such an expansion is carried out in §§3 and 4 for a smooth defect profile of the form $u_0 = y + \epsilon \tanh(y)$, and the suggestion is verified. Indeed, the analysis yields a complete description of the unstable eigenfunctions and their growth rates. In addition, as shown in the Appendix, the expansions of both the eigenfunctions and the dispersion relation in powers of k, converge for small ϵ. These results significantly generalize Gill's (1965) asymptotic analysis of the neutral mode. Finally, a brief discussion of the induced mean flow generated by the instability and the role of critical layers is presented in §5. Our conclusions follow in §6.

2. Discrete models

In this section, we consider two discrete profiles containing a defect. The first profile is discontinuous at $y = 0$, corresponding to a vortex sheet at the origin, but the amplitude of the discontinuity is small. The second profile is continuous, but has discontinuities in the first derivative. Both problems can be solved by elementary

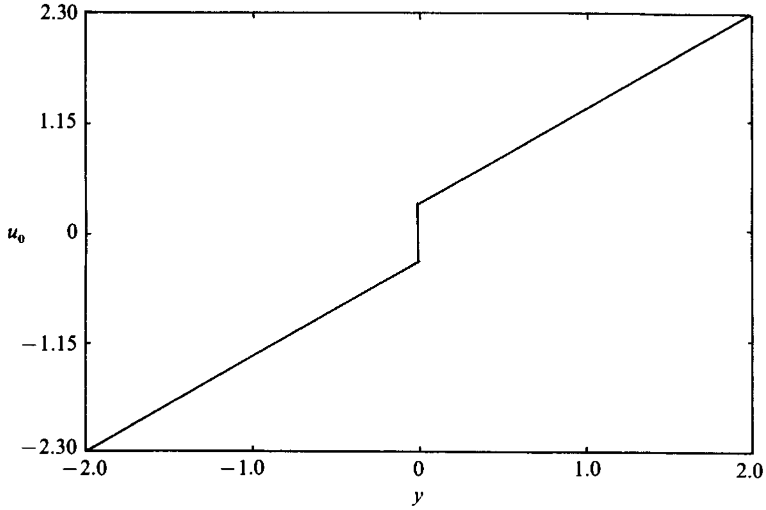

FIGURE 1. The shear profile $u_0(y) = y+\epsilon[\theta(y)-\theta(-y)]$ for $\epsilon = 0.3$.

methods (Drazin & Reid 1981), and the solutions are used to motivate the analysis undertaken in §3.

Model A

The first model consists of a Kelvin–Helmholtz defect in a mean flow,

$$u_0 = y+\epsilon\,[\theta(y)-\theta(-y)], \tag{2.1}$$

where θ is the step function. This shear profile is shown in figure 1. The solution of the Rayleigh equation is obtained by constructing explicit solutions in the half-planes $y > 0$ and $y < 0$, and imposing the jump conditions

$$[(u_0-c)\,\phi'-u_0'\,\phi]_-^+ = 0, \tag{2.2a}$$

and

$$\left[\frac{\phi}{u_0-c}\right]_-^+ = 0, \tag{2.2b}$$

at $y = 0$. Since $u_0'' = 0\,(y \neq 0)$, the solutions take the form

$$\phi^\pm = a^\pm\,\mathrm{e}^{\mp ky} \quad (y \gtrless 0). \tag{2.3}$$

Applying the jump conditions (2.2) to eliminate the constants $a^\pm$ yields the dispersion relation

$$c^2 = -\frac{\epsilon}{k}-\epsilon^2. \tag{2.4}$$

The dispersion relation is non-analytic at $k = 0$. This functional dependence will be found to persist in the smooth profile discussed in §3. The physical reason behind the divergence as $k\to 0$ is quite simple. The vortex sheet at $y = 0$ responsible for the velocity discontinuity is unstable in the absence of mean shear to spatially periodic disturbances with wavenumbers k in the flow direction. The effect of the mean part of u_0, i.e. the linear profile $u_0 = y$, is to spin up (or down) the resulting vortices via advection. The smaller the longitudinal wavenumber k, the larger the vortices become, as is readily seen from (2.3), and the larger are the velocities shearing them. Consequently, c diverges as $k\to 0$.

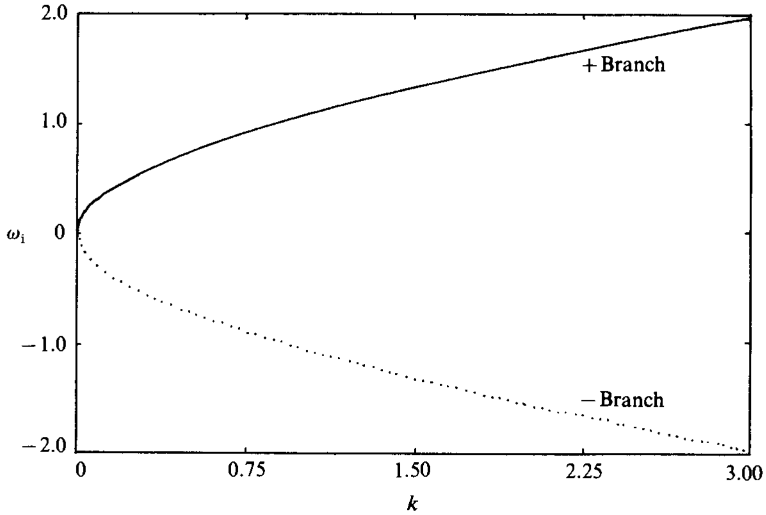

FIGURE 2. The growth rate ω_i as a function of longitudinal wavenumber k for $\epsilon = +0.1$ for the shear profile type shown in figure 1.

For $\epsilon > 0$, the frequency $\omega(\equiv kc)$ is purely imaginary, and the system is unstable for any ϵ. The resulting growth rate ω_i is shown in figure 2. In this case, the instability is stationary and does not propagate. For $\epsilon < 0$, the behaviour is quite different. From (2.4) we find

$$\omega^2 = |\epsilon| k(1-|\epsilon| k). \tag{2.5}$$

This dispersion relation is shown in figures 3 and 4. For $k < 1/|\epsilon|$, the mean shear is stabilizing and ω is purely real; the perturbations take the form of neutrally stable travelling waves. For $c > 0$, we find that:

$$\frac{d\omega}{dk} > 0 \quad \text{in } 0 < k < \frac{1}{2|\epsilon|}, \tag{2.6a}$$

$$\frac{d\omega}{dk} < 0 \quad \text{in } \frac{1}{2|\epsilon|} < k < \frac{1}{|\epsilon|}. \tag{2.6b}$$

A similar split occurs on the other branch of the dispersion relation, where $c < 0$. Thus, depending on k, the envelope and the phase may propagate in the same, or in opposite directions. Those wavenumbers satisfying $k > 1/|\epsilon|$ are all unstable. This is the vestige of the Kelvin–Helmholtz instability.

Model B

To obtain a more realistic model, one must allow the shear layer to have finite thickness. In this section we therefore consider the profile

$$u_0 = y + \epsilon\{[\theta(y-1) - \theta(-y-1)] + y[\theta(y+1) - \theta(y-1)]\} \tag{2.7}$$

sketched in figure 5. The solutions of the Rayleigh equation now take the form

$$\phi = \begin{cases} a\,e^{-ky} & (y > 1), \\ b\,e^{ky} + d\,e^{-ky} & (-1 < y < 1), \\ f e^{ky} & (y < -1). \end{cases} \tag{2.8}$$

Imposing the matching conditions at $y = \pm 1$ yields four homogeneous linear

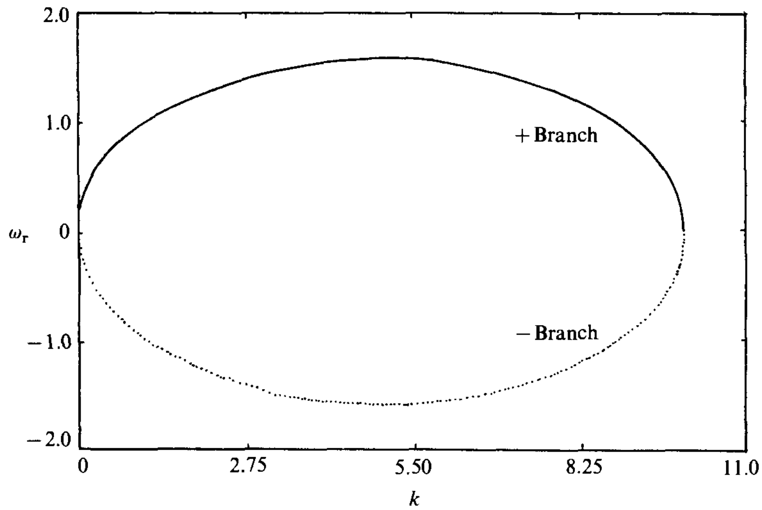

FIGURE 3. The frequency ω_r as a function of longitudinal wavenumber k for $\epsilon = -0.1$ for the shear profile type shown in figure 1.

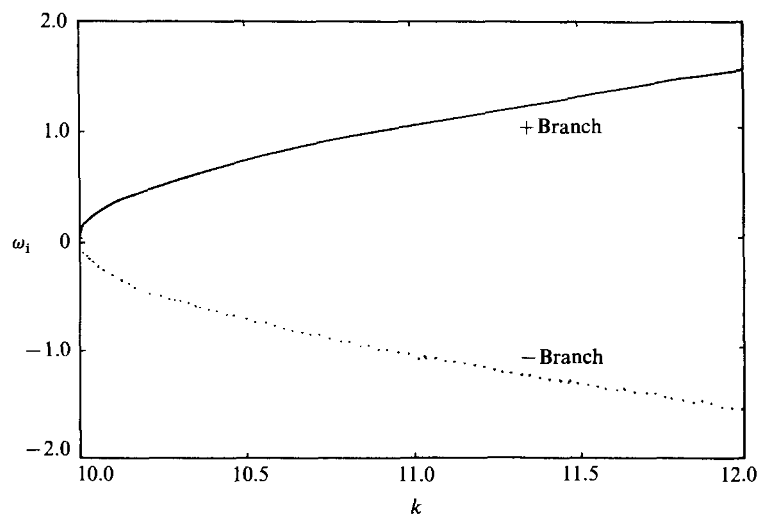

FIGURE 4. The growth rate ω_i as a function of longitudinal wavenumber k for $\epsilon = -0.1$ for the shear profile type shown in figure 1.

equations for the four unknowns a, b, d, f. The solvability condition yields the dispersion relation

$$c^2 = \frac{1}{4k^2}[\epsilon^2(1-e^{-4k}) - 4\epsilon k(1+\epsilon) + 4k^2(1+\epsilon)^2]. \tag{2.9}$$

We show the real and imaginary parts of $\omega = ck$ in figures 6 and 7 for $\epsilon > 0$.

The dispersion relation (2.9) has the following properties. When $\epsilon > 0$, and k is sufficiently large, $c^2 > 0$. All such solutions represent neutrally stable, travelling waves. As $k \to 0$, $c^2 \to -\epsilon/k$ in agreement with model A. It follows that there must

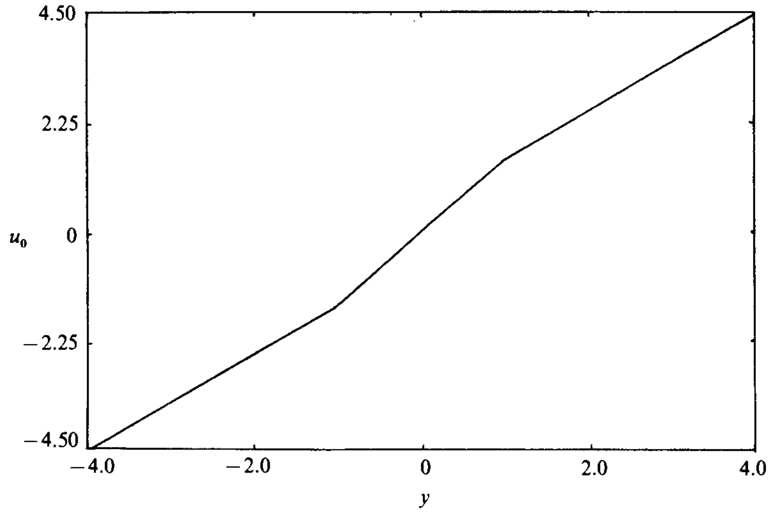

FIGURE 5. The discrete finite shear profile ($\epsilon = 0.5$)
$u_0 = y + \epsilon\{[\theta(y-1) - \theta(-y-1)] + y[\theta(y+1) - \theta(y-1)]\}$.

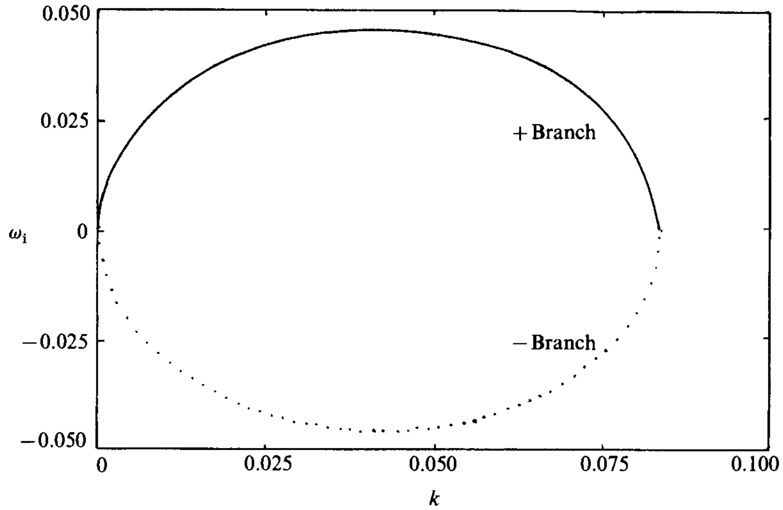

FIGURE 6. The growth rate ω_i as a function of longitudinal wavenumber k for $\epsilon = 0.1$ for the shear profile type shown in figure 5.

exist a neutral wavenumber satisfying $c(k_0) = 0$. To estimate the bandwidth of the instability, $0 < k < k_0$, we expand the bracket in (2.9) in powers of k to obtain

$$\omega^2 = k[-\epsilon + k(1 + 2\epsilon - \epsilon^2) + \tfrac{8}{3}k^2\epsilon^2 + O(k^3\epsilon^2)]. \qquad (2.10)$$

At the band edge k_0, the frequency vanishes. It is simple to show that there is exactly one such value of k_0 and that it is $O(\epsilon)$. To leading order

$$k_0 = \epsilon(1 - 2\epsilon) + O(\epsilon^3). \qquad (2.11)$$

The maximum growth rate occurs at $\tfrac{1}{2}k_0$ and is given by

$$\omega_{i_{max}} = \tfrac{1}{2}\epsilon(1-\epsilon). \qquad (2.12)$$

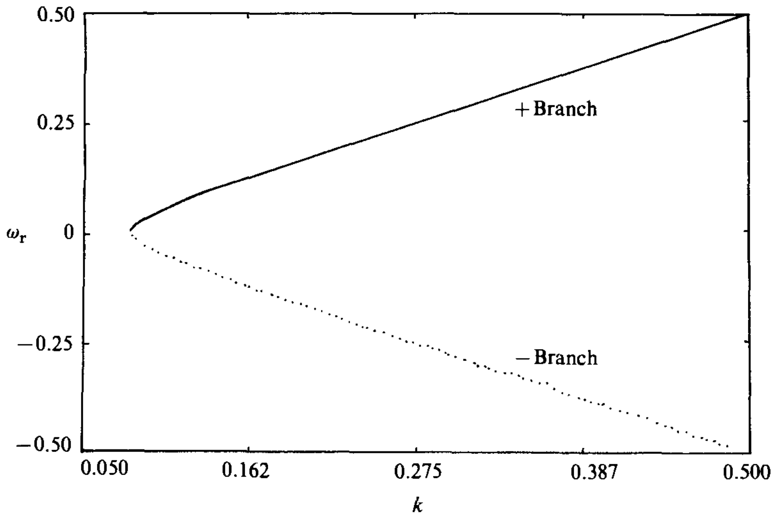

FIGURE 7. The frequency ω_r as a function of longitudinal wavenumber k for $\epsilon = 0.1$ for the shear profile type shown in figure 5.

In contrast to these results we recall that in the absence of the ambient linear shear the band edge occurs at $k_0 = O(1)$, while the growth rate is $O(\epsilon)$. Thus the effect of the linear shear is to squeeze the band of unstable wavenumbers down to $O(\epsilon)$ without decreasing the growth rate from what it would be in its absence. Since ϵ is a fixed, externally imposed parameter, all unstable wavenumbers satisfy $k \leqslant O(\epsilon)$. The wavenumber k thus becomes a natural small expansion parameter for fixed $\epsilon \ll 1$. One can, however, do much better, since one may carry out a double expansion in both k and ϵ. The resulting long-wave expansion (LWE) is not only simplified by the presence of $\epsilon \ll 1$, but its validity now extends over the whole band of unstable wavenumbers. It is this procedure that is applied to a profile with a smooth defect in the following section.

3. The long-wave expansion

In this section we study a continuous profile with a defect, which we take to be

$$u_0 = y + \epsilon \tanh y. \tag{3.1}$$

This profile has an inflexion point and so satisfies Rayleigh's necessary condition for instability. In the absence of the linear shear the bandwidth of the instability is $O(1)$ (Michalke 1964). As indicated in the preceding section it is reasonable to surmise that this is no longer the case in the presence of the linear shear.

To solve Rayleigh's equation (1.1) with the profile (3.1) we employ the long-wave expansion (Drazin & Howard 1962). On an unbounded domain, this is a uniform perturbation in k only after the correct asymptotic behaviour as $y \to \pm\infty$ has been factored out. Since $u_0'' \to 0$ as $y \to \pm\infty$, we have $\phi'' \to k^2\phi$ as $y \to \pm\infty$. We differ slightly from standard procedure and factor out the asymptotic behaviour by looking for solutions of the form

$$\phi^{\pm}(y) = \chi^{\pm}(y)\, \Psi^{\pm}(y) \exp(\mp ky), \tag{3.2a}$$

where
$$\Psi^{\pm}(y) \equiv w(y) \int_{\pm\infty}^{y} \frac{\mathrm{d}r}{w^2(r)}, \tag{3.2b}$$
and
$$w(y) \equiv u_0(y) - c. \tag{3.2c}$$

Here the $\pm$ signs refer to the regions $y \gtrless 0$, respectively. Note that for unstable modes the phase speed c is complex and hence $\Psi^{\pm}$ is well defined. In addition, $|\Psi^{\pm}| \to 1$ as $y \to \pm\infty$, so that the correct asymptotic behaviour is included in the explicit exponential decay. Our task is to determine the functions $\chi^{\pm}(y)$ in terms of a uniform expansion in k.

We proceed, as usual, by expanding $\chi^{\pm}$:
$$\chi^{\pm}(y) = 1 + \sum_{n=1}^{\infty} k^n f_n^{\pm}(y) \equiv 1 + f^{\pm}. \tag{3.3}$$

Substituting equations (3.1)–(3.3) into (1.1) and separating orders in k yields a recursion relation for the $f_n^{\pm}$ of the form
$$(\Psi^{\pm^2} f_{n+1}^{\pm\prime}(y))' = \pm 2\Psi^{\pm}(\Psi^{\pm} f_n^{\pm})', \tag{3.4}$$
subject to the conditions $f_0^{\pm} = 1$, and $f_n^{\pm\prime}(\pm\infty) = 0$. The first two solutions are
$$f_1^{\pm} = \pm \int_{\pm\infty}^{y} \mathrm{d}r \left[1 - \frac{1}{\Psi^{\pm^2}(r)}\right], \tag{3.5a}$$
and
$$f_2^{\pm} = \pm 2 \int_{\pm\infty}^{y} \frac{\mathrm{d}r}{\Psi^{\pm^2}(r)} \int_{\pm\infty}^{r} \mathrm{d}s\, \Psi^{\pm}(\Psi^{\pm} f_1^{\pm})'. \tag{3.5b}$$

It is possible to formally establish the convergence of the expression (3.3) and to estimate the radius of convergence in k, as shown in the Appendix. The resulting expressions for $\phi^{\pm}$ do not solve Rayleigh's equation unless the dispersion relation obtained by imposing continuity on ϕ and ϕ' is satisfied. This dispersion relation is obtained and analysed in the following section.

4. Derivation of the dispersion relation

The dispersion relation is obtained from the requirement that ϕ and ϕ' are continuous across $y = 0$. The final result does not depend on the value of y at which the matching conditions are imposed. Since the $\phi^{\pm}$ are defined up to an unknown normalization, we obtain
$$\chi^{+}(0)\,\Psi^{+}(0) = M\chi^{-}(0)\,\Psi^{-}(0), \tag{4.1a}$$
and
$$(\chi^{+}\Psi^{+})'(0) - k(\chi^{+}\Psi^{+})(0) = M[(\chi^{-}\Psi^{-})'(0) + k(\chi^{-}\Psi^{-})(0)]. \tag{4.1b}$$

Here M is the constant of proportionality. Eliminating M from (4.1) yields
$$(\chi^{-}\Psi^{-})(0)\,(\chi^{+}\Psi^{+})'(0) - (\chi^{+}\Psi^{+})(0)\,(\chi^{-}\Psi^{-})'(0) = 2k(\chi^{+}\Psi^{+})(0)(\chi^{-}\Psi^{-})(0), \tag{4.2}$$
which may be rewritten, with the aid of expansions (3.2) and (3.3), in the form
$$\sum_{n=0}^{\infty} A_n(\epsilon, c)\, k^n = 0. \tag{4.3}$$

The coefficients A_n are given by the following expressions:

$$A_0 = \int_{-\infty}^{+\infty} \frac{\mathrm{d}r}{w^2(r)}, \tag{4.4a}$$

$$A_1 = A_0[f_1^+(0)+f_1^-(0)] + (\Psi^+\,\Psi^-)(0)\,[f_1^{+\prime}(0)-f_1^{-\prime}(0)-2], \tag{4.4b}$$

$$A_2 = A_0[f_2^+(0)+f_2^-(0)+f_1^-(0)f_1^+(0)] + (\Psi^+\,\Psi^-)(0)\,[f_2^{+\prime}(0)-f_2^{-\prime}(0) + f_1^-(0)f_1^{+\prime}(0)-f_1^+(0)f_1^{-\prime}(0)-2f_1^+(0)-2f_1^-(0)], \tag{4.4c}$$

and

$$A_n = A_0\left(\sum_{k=0}^{n} f_k^+(0)f_{n-k}^-(0)\right) + (\Psi^+\,\Psi^-)(0) \times\left\{\sum_{k=0}^{n}[f_{n-k}^{+\prime}(0)f_k^-(0)-f_{n-k}^{-\prime}(0)f_k^+(0)] - 2\sum_{k=0}^{n-1} f_{n-k-1}^+(0)f_k^-(0)\right\} \quad (n \geqslant 1). \tag{4.4d}$$

For the profile (3.1), $u_0(y)$ is antisymmetric, and hence equation (1.1) is invariant under the transformation $y \to -y$, $c \to -c^*$, and $\phi \to \phi^*$ (Tatsumi & Gotoh 1960). Since this maps an unstable mode at a given k onto another unstable mode, uniqueness of the solution requires that $c = -c^*$ and $\phi(y) = \phi^*(-y)$. Hence, $\mathrm{Re}\,(c) = 0$. This is not the case when $u_0(y)$ is not antisymmetric. We next expand the A_n in powers of ϵ. This serves to simplify the analytical expressions that need to be evaluated. We present the details of the procedure for A_0. Expanding the integrand in powers of ϵ, we obtain

$$A_0 = \int_{-\infty}^{\infty}\frac{\mathrm{d}r}{w^2} = \int_{-\infty}^{\infty}\frac{\mathrm{d}r}{(r-\mathrm{i}c_\mathrm{i})^2}\left[1-\epsilon\frac{2\tanh r}{(r-\mathrm{i}c_\mathrm{i})}+3\epsilon^2\frac{\tanh^2 r}{(r-\mathrm{i}c_\mathrm{i})^2}+O(\epsilon^3)\right]. \tag{4.5}$$

The first integral vanishes. Integrating by parts twice at $O(\epsilon)$ and three times at $O(\epsilon^2)$ yields

$$A_0 = 2\epsilon\int_{-\infty}^{\infty}\mathrm{d}r\frac{r\tanh r\,\mathrm{sech}^2 r}{r^2+c_\mathrm{i}^2} + \tfrac{1}{2}\epsilon^2\int_{-\infty}^{\infty}\mathrm{d}r\frac{r\,(\tanh r)'''}{r^2+c_\mathrm{i}^2}+O(\epsilon^3). \tag{4.6}$$

Applying the same analysis to the $O(k)$ term in (4.3), one obtains

$$A_1 = -2+O(\epsilon^2). \tag{4.7}$$

The expansion (4.3) may be proved convergent. The necessary analysis may be found in the Appendix. This fact does not, however, establish how rapidly the series converges. That is, we do not know at what point we may truncate (4.3) and still obtain a credible approximation to the full series. We now show that $A_2 = O(\epsilon^2)$, to leading order, suggesting that a low-order truncation of the dispersion relation may be accurate. We proceed by noting that

$$\Psi^\pm + 1 = \epsilon\,\mathrm{sech}^2(y) - \epsilon(y-\mathrm{i}c_\mathrm{i})\int_{\pm\infty}^{y}\mathrm{d}r\frac{(\tanh r)''}{(r-\mathrm{i}c_\mathrm{i})}+O(\epsilon^2). \tag{4.8}$$

Applying (4.8) to (3.5a), we see that $f_1^\pm$ and $f_1^{\pm\prime}$ are both $O(\epsilon)$. It follows that $f_2^\pm$ and $f_2^{\pm\prime}$ are also $O(\epsilon)$. In addition, from (4.6), $A_0 = O(\epsilon)$. It follows that $A_2 = A_2^{(1)}\,\epsilon + O(\epsilon^2)$, where

$$A_2^{(1)} \equiv \lim_{\epsilon\downarrow 0}\frac{1}{\epsilon}[f_2^{+\prime}(0)-f_2^{-\prime}(0)-2f_1^+(0)-2f_1^-(0)]. \tag{4.9}$$

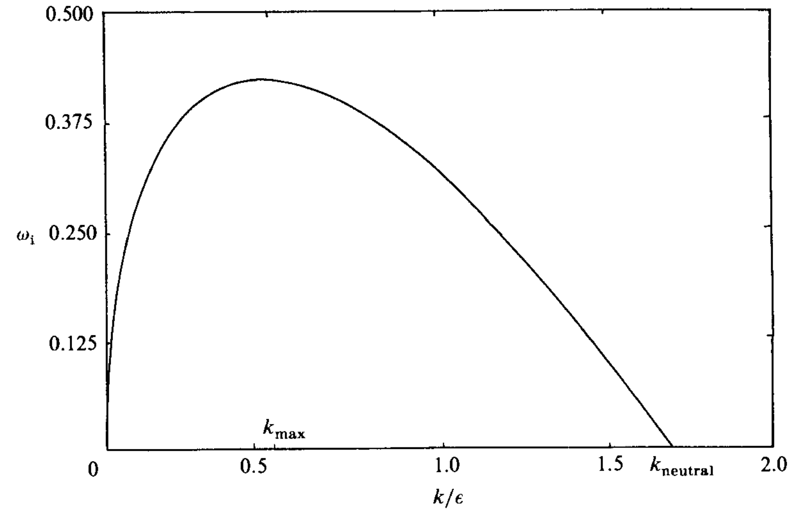

FIGURE 8. The growth rate ω_i was a function of longitudinal wavenumber k/ϵ for the dispersion relation (4.12) obtained via the LWE for profile (3.1).

Applying expansion (4.8) to (3.5), we obtain

$$f_1^+(0)+f_1^-(0) = 2\epsilon\int_0^\infty \mathrm{d}r\left[(r-\mathrm{i}c_i)\int_r^\infty \mathrm{d}y\frac{\operatorname{sech}^2 y}{(y-\mathrm{i}c_i)^2}+\text{c.c.}\right]+O(\epsilon^2), \qquad (4.10a)$$

and

$$f_2^{\pm\prime}(0) = \pm f_1^\pm(0)+\frac{1}{\Psi^{\pm 2}(0)}\int_{\pm\infty}^0 \mathrm{d}r\,(\Psi^\pm-1)\,(\Psi^\pm+1). \qquad (4.10b)$$

Substituting these results into (4.9), we find that

$$A_2^{(1)} \equiv 0. \qquad (4.11)$$

We conclude that $A_2 = O(\epsilon^2)$.

To leading order in k and ϵ, equations (4.3)–(4.7) yield

$$\epsilon\int_{-\infty}^\infty \mathrm{d}r\frac{r\tanh r\operatorname{sech}^2 r}{r^2+c_i^2} = k+O(\epsilon^2). \qquad (4.12)$$

This equation determines the growth rate $\omega_i \equiv kc_i$ as a function of k, as shown in figure 8. Note that the integral in (4.12) exists for all c_i, including $c_i = 0$, and so is $O(1)$. Therefore, for the instability, $k = O(\epsilon)$, in agreement with our results for the profile B. To determine the neutral wavenumber k_0, we may set $c_i = 0$ in (4.12). We obtain $k_0 = 1.705\epsilon$.

A direct comparison may be made between the above, systematic result and Gill's (1965) asymptotic theory. His equation (2.10) is readily extended to a channel whose boundaries are at $y = \pm R$ rather than $y = \pm 1$ yielding

$$a\int_{-\infty}^\infty \mathrm{d}r\frac{ru_0''}{r^2+\beta^2} = -2\,k\coth(kR), \qquad (4.13)$$

where in Gill's notation, a is the amplitude of the defect imposed upon the Couette flow, and $c = \mathrm{i}\epsilon'\beta$, ϵ' being the dimensionless width of the defect and β a number of

$O(1)$. Setting $c = 0$, we see that this predicts a threshold amplitude for instability which behaves as

$$\frac{-2}{R\int_{-\infty}^{\infty} \mathrm{d}r\left(\frac{u_0''}{r}\right)}.$$

Thus at large R, but long wavelengths ($kR \ll 1$), the amplitude threshold becomes arbitrarily small, in agreement with our calculation. Note, however, that (4.13) also applies for $k = O(1)$.

As $k \to 0$, equation (4.12) indicates that $c_i \to \infty$. To demonstrate this, we rewrite (4.12) with respect to the integration variable $v = r/c_i$, obtaining

$$\epsilon\int_{-\infty}^{\infty} \mathrm{d}v \frac{v \tanh (c_i v) \operatorname{sech}^2 (c_i v)}{(1+v^2)} = k + O(\epsilon^2). \tag{4.14}$$

As $c_i \to \infty$, the integrand contributes only for $|v| \lesssim 1/c_i$. We may therefore expand $1/(1+v^2)$ in powers of v to obtain an expansion for the integral in inverse powers of c_i. The leading-order contribution results from replacing $1+v^2$ in the denominator by 1. Equation (4.14) then becomes

$$-\frac{\epsilon}{2c_i^2}\int_{-\infty}^{\infty} \mathrm{d}r\, r\frac{\mathrm{d}}{\mathrm{d}r}\operatorname{sech}^2 r = k, \tag{4.15}$$

which, following an integration by parts, yields $c_i^2 = \epsilon/k$. This is in complete agreement with the results of §2.

Two features of the approximate dispersion relation (4.12) deserve comment. The curve $\omega_i(k)$ plotted in figure 8 looks qualitatively like that for model B. It displays a well-defined, maximum growth rate occurring at $k = k_m$. The slope $\omega_i'(k_0)$ is finite for the smooth profile in contrast to the discrete profile B, where it is infinite, an effect that is known to occur in the absence of the mean shear [Maslowe 1981]. Secondly, the quantity $c_m = \omega_i(k_m)/k_m$ is independent of the defect strength, ϵ, to leading order in ϵ. To show this, we rewrite (4.12) as $\epsilon F(\omega_i/k) = k$. Differentiating with respect to k, and setting $\omega_i'(k) = 0$ to fix k at k_m, we obtain $c_m F'(c_m) = -k_m/\epsilon$. Eliminating the right-hand side of this equation using the above form of (4.12) yields $c_m F'(c_m) = -F(c_m)$. This equation for c_m is independent of ϵ, to leading order in ϵ, and remains valid as $\epsilon \to 0^+$. From figure 8, it follows that $c_m = O(1)$, and hence that $\omega_i(k_m) \approx k_m$.

5. Induced mean flow

The Reynolds stresses produced by a growing shear-flow instability modify the unstable shear profile (Huerre 1980, 1987). In the absence of a nonlinear theory describing the equilibration of the instability, we confine ourselves here to a calculation of the induced mean flow that is valid for short times only. Starting with the two-dimensional, incompressible Euler equations, one can readily show (Drazin & Reid 1981) that to leading order in ϵ, the mean flow is of the form

$$u(y) = u_0(y) + \delta^2 u_2(y,t) + O(\delta^3), \tag{5.1}$$

where $$u_2(y,t) = -\tfrac{1}{2}\epsilon\,|\phi|^2(y)\exp(2kc_i t)\frac{\tanh y \operatorname{sech}^2 y}{y^2+c_i^2} \equiv v_2(y)\exp(2kc_i t), \tag{5.2}$$

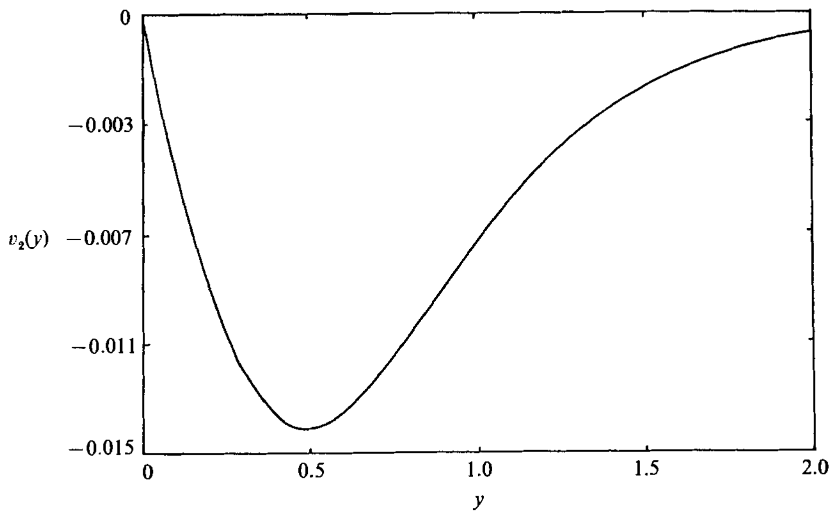

FIGURE 9. Induced mean flow $v_2(y)$ for $\epsilon = 0.1$, $k/\epsilon = 0.47$, for which $c_i = 0.9$.

and δ is the amplitude of the unstable mode with wavenumber k. The quantity $u_2(y)\exp(-2kc_i t)$ is shown in figure 9. Since $|\phi|^2(y) = |\phi|^2(-y)$ (see §4), the induced mean flow is an odd function of y.

Although the above analysis is valid only for short times, it is indicative of the processes responsible for the ultimate equilibration of the instability. We see that the induced mean flow decreases the maximum shear that occurs at $y = 0$, suggesting a decrease in the growth rate of the instability. An important point is that for small c_i the correction to the background shear becomes singular. Consequently, the correction is a strong function of the wavenumber k near k_0. This is a signature of the critical-layer effects associated with nearly neutral modes. In the limit $c_i \to 0^+$, the naïve perturbation theory fails, and it is necessary to include either the effects of viscosity or of nonlinearity (or both) to regularize this singularity (Davis 1969; Huerre 1980, 1987; Schade 1964; Stuart 1960; Watson 1960). In contrast, as $k \to 0$ ($c_i \to \infty$) the induced mean flow vanishes uniformly in y.

6. Discussion

Our understanding of the nonlinear behaviour of the Rayleigh equation is extensive for those systems for which the nearly neutral mode dominates the physics. The goal of a theory, however, should be to describe the dynamics of the most unstable mode. The purpose of the present work has been to make such modes directly accessible to the theory. Using the novel feature demonstrated for discretized models, that of $O(\epsilon)$ bandwidth of instability, we have re-examined the long-wave expansion for a smooth model of a defect in a mean shear flow. The presence of a second small parameter, ϵ, measuring the ratio of excess shear in the defect to the mean shear, not only restricts k to $k \leqslant O(\epsilon)$, but also permits a double expansion to be carried out, in both ϵ and k. This substantially extends the applicability of the LWE to smooth profiles. In particular, the technique readily extends to velocity profiles that are not antisymmetric in y. In capturing the most unstable wavenumbers, the present work overcomes the difficulties encountered in earlier applications of the LWE, where the most unstable wavenumbers are $O(1)$. Finally, the present work provides a systematic, non-asymptotic extension of the work of Gill (1965) to non-neutral modes.

All three models were found to behave alike in the limit of $k \to 0$. Those cases having finite shear thickness all behave as a Kelvin–Helmholtz defect. The presence of an unbounded uniform part of the shear generated a divergent phase speed as $k \to 0$. This divergence in c at small k can be explained on simple physical grounds as a spin up (or spin down) of the defect-induced vorticity by the strong uniform shear. For $\epsilon > 0$ the spin-up effect increases the growth rate of the instability, while for $\epsilon < 0$ the spin-down effect stabilizes the smallest wavenumbers. We find both travelling neutral modes and unstable stationary modes.

The presence of the small parameter, ϵ, facilitated obtaining the first two terms of the dispersion relation from the double expansion. Although we can show that both the expansion of the eigenfunctions and of the dispersion relation converge, the rate of convergence is difficult to assess. The fact that the coefficient A_2 of k^2 is already $O(\epsilon^2)$ suggests that the two leading terms of the expansion might yield quantitatively accurate results for sufficiently small ϵ. The difficulty is compounded, however, by the well-known fact (Bender & Orszag 1978) that adding small terms to a function can dramatically alter the locations of its zeros. A numerical study of this issue will be necessary.

These results give us confidence that we have correctly described the stability properties of the defect. Of these, of particular interest is the fact that for $\epsilon > 0$ the maximum growth rate of the instability, $\omega_i(k_m)$, is $O(\epsilon)$ as ϵ decreases to zero. This is a consequence of the fact that the longitudinal wavenumber k_m corresponding to the maximum growth decreases to zero linearly with ϵ while c_m remains $O(1)$. If we suppose that the defect is introduced into the background flow by a finite-amplitude perturbation of strength ϵ, we are led to conclude that a small but finite-amplitude perturbation will lead to a dynamical instability on a timescale $O(1/\epsilon)$, provided that the background shear will spin up the vorticity distribution generated by the defect. Thus, our calculation lends support to the widespread belief that unbounded Couette flow is subcritically unstable.

Although we have studied the temporal problem, it is known that spatially growing modes occur in experiments (Miksad 1972). For example, in a mixing layer driven by a harmonic source, ω must be real. In order to satisfy the dispersion relation, k may be forced to be complex. Thus the dispersion relation may have to be analytically continued to complex k and ω. For small $|k|$, the expansions provided here are, however, still valid.

The presence of the singular denominator in the expression for the induced mean flow u_2, together with the fact that $k = O(\epsilon)$, $\omega = O(\epsilon)$, and c_i varies between zero and infinity within the narrow band of unstable modes, introduces a series of spatial scales into the problem. For c_i very small, there appear to be three scales. There is the smallest scale $y \approx c_i$ due to the singular denominators, the $O(1)$ defect lengthscale, and the spatial decay lengthscale $y \approx 1/k \approx 1/\epsilon$. For the most unstable mode of the smooth shear profile, $c_i = O(1)$, while the eigenfunction lengthscale $1/k$ is still $O(1/\epsilon)$. Here, there are only two scales. Although the vorticity is confined to a layer of $O(1)$ thickness, the eigenfunction extends out over a much larger region. This supports the view taken by Gill (1965) in his asymptotic theory.

In conclusion, we have obtained what we believe to be the first, non-trivial, smooth profile for which a single application of the long-wave expansion is valid over the whole range of instability. This is useful since it provides a building block for extending the theory of shear flows at both the linearized and nonlinear level. The problem of developing a mode-coupled theory to study dynamics may become accessible via a Galerkin approximation relative to the above eigenfunctions. The goal would be to understand the tendency of free shear flows to evolve toward large, finite-amplitude vortices. That such solutions exist has been shown by Stuart (1967).

We would like to acknowledge financial support from the California Space Institute under grants CS 14-84 and CS 61-85, and to thank Professor C. F. McKee for providing additional support and funding. We have benefited from discussions with Professors J. Neu and J.-P. Zahn. We thank Professor J. T. Stuart of Imperial College for bringing the paper by Gill to our attention.

Appendix. Convergence properties of the expansion

A.1. *Convergence of the eigenfunction expansion*

To study convergence of the LWE, we follow the approach taken by Drazin & Howard (1962). We begin by obtaining bounds on $|\Psi^{\pm}|$. From §4, we have $c_r = 0$. Since we are considering unstable modes, ϵ and c_i are positive. We proceed as follows:

$$|\Psi^{\pm}| = |w| \left| \int_{\pm\infty}^{y} \frac{\mathrm{d}r}{w^2} \right| = |w| \left| \int_{\infty}^{u} \frac{\mathrm{d}v}{1+\epsilon\,\mathrm{sech}^2 r(v)} \frac{1}{(v-\mathrm{i}c_i)^2} \right|$$

$$= |w| \left| \int_{\pm\infty}^{u} \frac{\mathrm{d}v}{(v-\mathrm{i}c_i)^2} \left[1 - \epsilon \frac{\mathrm{sech}^2 r(v)}{1+\epsilon\,\mathrm{sech}^2 r(v)} \right] \right| \equiv |w|\,|a^{\pm} - b^{\pm}|, \quad \text{(A 1)}$$

where $r + \epsilon \tanh(r) = v$ determines $r(v)$ in the integrand. Using the inequality $||a| - |b|| \leqslant |a-b| \leqslant |a| + |b|$, we have

$$L^{\pm} \equiv |w| \left| \left| \int_{\pm\infty}^{u} \frac{\mathrm{d}v}{(v-\mathrm{i}c_i)^2} \right| - \epsilon \left| \int_{\pm\infty}^{u} \frac{\mathrm{d}v}{(v-\mathrm{i}c_i)^2} \frac{\mathrm{sech}^2 r(v)}{1+\epsilon\,\mathrm{sech}^2 r(v)} \right| \right|$$

$$\leqslant |\Psi^{\pm}| \leqslant |w| \left| \left| \int_{\pm\infty}^{u} \frac{\mathrm{d}v}{(v-\mathrm{i}c_i)^2} \right| + \epsilon \left| \int_{\pm\infty}^{u} \frac{\mathrm{d}v}{(v-\mathrm{i}c_i)^2} \frac{\mathrm{sech}^2 r(v)}{1+\epsilon\,\mathrm{sech}^2 r(v)} \right| \right| \equiv U^{\pm}, \quad \text{(A 2)}$$

where $L^{\pm}$ and $U^{\pm}$ refer to lower and upper bounds on $|\Psi^{\pm}|$. Note that the superscript $\pm$ restricts y to $y \gtrless 0$.

Since $\mathrm{sech}^2 r(v) \leqslant 1$, we have the following upper bound for $|b|$:

$$|b^{\pm}| \leqslant \epsilon \left| \int_{\pm\infty}^{u} \frac{\mathrm{d}v}{v^2 + c_i^2} \right|. \quad \text{(A 3)}$$

Using (A 3), we find a lower bound to $L^{\pm}$ and an upper bound to $U^{\pm}$:

$$|w| \left| \left| \int_{\pm\infty}^{u} \frac{\mathrm{d}v}{(v-\mathrm{i}c_i)^2} \right| - \epsilon \left| \int_{\pm\infty}^{u} \frac{\mathrm{d}v}{v^2+c_i^2} \right| \right| \leqslant L^{\pm} \leqslant |\Psi^{\pm}| \leqslant U^{\pm}$$

$$\leqslant |w| \left| \left| \int_{\pm\infty}^{u} \frac{\mathrm{d}v}{(v-\mathrm{i}c_i)^2} \right| + \epsilon \left| \int_{\pm\infty}^{u} \frac{\mathrm{d}v}{v^2+c_i^2} \right| \right| \quad \text{(A 4)}$$

The above inequalities become

$$1 - \epsilon |w| \int_{|u|}^{\infty} \frac{\mathrm{d}v}{v^2+c_i^2} \leqslant |\Psi^{\pm}| \leqslant 1 + \epsilon |w| \int_{|u|}^{\infty} \frac{\mathrm{d}v}{v^2+c_i^2}, \quad \text{(A 5)}$$

where the symmetry of the integrand has been exploited to restrict the range of integration to positive values. The integral satisfies

$$(u^2+c_i^2)^{\frac{1}{2}}\int_{|u|}^{\infty}\frac{\mathrm{d}v}{v^2+c_i^2}<\frac{(u^2+c_i^2)^{\frac{1}{2}}}{|u|+c_i}<2. \tag{A 6}$$

We thus have
$$1-2\epsilon\leqslant|\Psi^{\pm}|\leqslant 1+2\epsilon. \tag{A 7}$$

To prove convergence of the series for $f^{\pm}$ (see (3.3)), we will construct a majorizing sequence for $f^{\pm\prime}$, and establish uniform convergence. The function $f^{\pm}$ is then obtained using term by term integration. We consider f^{+} and Ψ^{+}, restricting ourselves to $y>0$. The proof is essentially identical for f^{-} and Ψ^{-}. To proceed, define

$$\bar{\Psi}^{+}(\eta)\equiv\Psi^{+}(y), \tag{A 8a}$$

$$\bar{f}_n^{+}(\eta)\equiv f_n^{+}(y), \tag{A 8b}$$

where $\eta\equiv\exp(-y)$. We recall that $f_0\equiv 1$ and for $n\neq 0$, $f_n^{+}(\infty)=0$ and $f_n^{+\prime}(\infty)=0$. With the prime denoting $\mathrm{d}/\mathrm{d}\eta$, one obtains ($n\geqslant 1$) from (3.4)

$$\begin{aligned}\bar{f}_{n+1}^{+\prime}(\eta)&=-\frac{2}{\eta\bar{\Psi}^{+2}}\int_0^{\eta}\mathrm{d}s\,\bar{\Psi}^{+}(\bar{\Psi}^{+}\bar{f}_n^{+})'\\&=-\frac{1}{\eta}\left[\int_0^{\eta}\mathrm{d}s\bar{f}_n^{+\prime}+\frac{1}{\bar{\Psi}^{+2}}\int_0^{\eta}\mathrm{d}s\,\bar{\Psi}^{+2}\bar{f}_n^{+\prime}\right].\end{aligned} \tag{A 9}$$

We define $\bar{f}_n^{+\prime}\equiv\gamma_n(\eta)$. Equation (A 9) then becomes

$$\begin{aligned}|\gamma_{n+1}|&\leqslant\frac{1}{\eta}\left[\int_0^{\eta}\mathrm{d}s|\gamma_n|+\frac{1}{(\min|\bar{\Psi}^{+}|^2)}\int_0^{\eta}\mathrm{d}s(\max|\bar{\Psi}^{+}|^2)|\gamma_n|\right]\\&<\frac{1}{\eta}\left[1+\left(\frac{1+2\epsilon}{1-2\epsilon}\right)^2\right]\int_0^{\eta}\mathrm{d}s|\gamma_n|\equiv\frac{\sigma}{\eta}\int_0^{\eta}\mathrm{d}s|\gamma_n|,\end{aligned} \tag{A 10}$$

where we have used (A 7), and the integrand is a function of s.

To apply (A 10), we first consider $n=0$. Since $\bar{f}_0\equiv 1$, it follows that

$$\gamma_1\equiv\bar{f}_1^{+\prime}=-\frac{2}{\eta\bar{\Psi}^{+2}}\int_0^{\eta}\mathrm{d}s\,\bar{\Psi}^{+}\bar{\Psi}^{+\prime}=-\frac{1}{\eta}\left[\frac{(\bar{\Psi}^{+}-1)(\bar{\Psi}^{+}+1)}{\bar{\Psi}^{+2}}\right], \tag{A 11}$$

where we have used the fact that $\bar{\Psi}^{+2}(0)=1$. Equation (A 11) is potentially singular only as $\eta\rightarrow 0$. To show that this limit is also well defined, we note that $(\bar{\Psi}^{+}-1)=-2+O(\epsilon)$ and $\bar{\Psi}^{+2}=1+O(\epsilon)$. The quantity $(\bar{\Psi}^{+}+1)/\eta$ becomes, using (A 1):

$$\frac{\bar{\Psi}^{+}+1}{\eta}=-\epsilon w(y)\,\mathrm{e}^{y}\int_{+\infty}^{u(y)}\frac{\mathrm{d}v}{(v-\mathrm{i}c_i)^2}\frac{\operatorname{sech}^2r(v)}{1+\epsilon\operatorname{sech}^2r(v)}, \tag{A 12}$$

with the result

$$\begin{aligned}\left|\frac{\bar{\Psi}^{+}+1}{\eta}\right|&\leqslant\epsilon|w|\mathrm{e}^{y}\left|\int_{\infty}^{u}\frac{\mathrm{d}v}{(v-\mathrm{i}c_i)^2}\frac{\operatorname{sech}^2r(v)}{1+\epsilon\operatorname{sech}^2r(v)}\right|\\&\leqslant 4\epsilon\,\mathrm{e}^{2\epsilon}|w|\mathrm{e}^{y}\int_u^{\infty}\mathrm{d}v\frac{\mathrm{e}^{-2v}}{v^2+c_i^2}.\end{aligned} \tag{A 13}$$

Here the last inequality follows using $y > 0$ and $\operatorname{sech}^2 r \leqslant 4\,\mathrm{e}^{-2r} = 4\,\mathrm{e}^{-2(v-\epsilon\tanh(r))} < 4\,\mathrm{e}^{-2v}\,\mathrm{e}^{+2\epsilon}$. Equation (A 13) simplifies, since

$$|w|\,\mathrm{e}^{y}\int_u^\infty \mathrm{d}v\frac{\mathrm{e}^{-2v}}{v^2+c_i^2} \leqslant |w|\,\mathrm{e}^{y}\,\mathrm{e}^{-2u(y)}\int_u^\infty \mathrm{d}v\frac{1}{v^2+c_i^2} < 2|w|\,\mathrm{e}^{-y}\int_u^\infty\frac{\mathrm{d}v}{(v+c_i)^2} < 2\eta. \quad \text{(A 14)}$$

We conclude that

$$\left|\frac{\bar{\Psi}+1}{\eta}\right| \leqslant 8\epsilon\,\mathrm{e}^{2\epsilon}\,\eta. \quad \text{(A 15)}$$

Combining this result with (A 11) yields

$$|\gamma_1| \leqslant \frac{(1+\epsilon)}{(1+2\epsilon)^2}16\epsilon\,\mathrm{e}^{2\epsilon}\eta \equiv \beta(\epsilon)\,\eta. \quad \text{(A 16)}$$

Iterating (A 10), we obtain

$$|\gamma_n| < (\tfrac{1}{2}\sigma)^{n-1}\beta(\epsilon)\,\eta < (\tfrac{1}{2}\sigma)^{n-1}\beta, \quad \text{(A 17)}$$

and hence

$$|\bar{f}^{+\prime}| \equiv |\Sigma\, k^n \bar{f}_n^{+\prime}| \leqslant \Sigma\, k^n |\bar{f}_n^{+\prime}|$$
$$\equiv \Sigma\, k^n|\gamma_n| < 2\frac{\beta}{\sigma}\Sigma\, k^n\,(\tfrac{1}{2}\sigma)^n. \quad \text{(A 18)}$$

This last series converges if and only if $|\frac{1}{2}k\sigma| < 1$ for $\epsilon \ll 1$. It is possible that the above analysis extends to $c_i = 0$. However, from equation (4.8), it is simple to show that $\Psi^{\pm}$ contains a logarithmic branch cut at $y = \mathrm{i}c_i$. In order to avoid potential singularities in the eigenfunctions or dispersion relation, we restrict our analysis to satisfy $c_i > 0$. By the Weierstrass comparison test, the series for $\bar{f}^{+\prime}$ converges uniformly. A sufficient condition for convergence is

$$k \leqslant \frac{2}{\sigma} = \frac{2}{1+\left(\dfrac{1+2\epsilon}{1-2\epsilon}\right)^2}. \quad \text{(A 19)}$$

Integrating term by by term yields a convergent expansion for $\bar{f}^{+}$. It must be evaluated on the dispersion relation to be a solution. Given the potential singularity at $c_i = 0$ at the neutral wavenumber k_0, the radius of convergence is taken to be

$$R = \min\left(\frac{2}{\sigma}, k_0\right). \quad \text{(A 20)}$$

Since $k_0 = O(\epsilon)$, $k_0 < 2/\sigma$ for ϵ sufficiently small. We have shown therefore that the eigenfunction expansion converges for all $k < k_0$.

A.2. *Convergence of the dispersion relation*

In order to establish convergence of (4.3), we need to bound $|A_n|$. This requires bounding $|f_n^{\pm}(0)|$ and $|f_n^{\pm\prime}(0)|$. We will use the bounds obtained in §A.1 to achieve this. To proceed, rewrite f_n^{+} and $f_n^{+\prime}$ in terms of η. Then $f_n^{+\prime}(y) = -\eta\bar{f}_n^{+\prime}(\eta)$. Since $y = 0$ becomes $\eta = 1$, we therefore have

$$f_n^{+}(0) = \bar{f}_n^{+}(1), \quad \text{(A 21a)}$$

and

$$f_n^{+\prime}(0) = -\bar{f}_n^{+\prime}(1). \quad \text{(A 21b)}$$

From (A 17) and (A 21), we now obtain

$$|f_n^{+\prime}(0)| \equiv |\gamma_n|(1) < (\tfrac{1}{2}\sigma)^{n-1}\beta. \tag{A 22a}$$

Since $\eta \in (0,1)$, $\bar{f}_n^{+}(0) = 0$, and by (A 17), $|\bar{f}_n^{+\prime}(\eta)| < (\tfrac{1}{2}\sigma)^{n-1}\beta$, we have

$$|f_n^{+}(0)| = |\bar{f}_n^{+}|(1) < (\tfrac{1}{2}\sigma)^{n-1}\beta. \tag{A 22b}$$

It is elementary to show that the same bounds hold if one replaces the + superscripts in (A 22) with $-$.

We proceed to bound (4.4d). For $n > 1$ we obtain

$$\begin{aligned}
|A_n| \leqslant |A_0|\left(\sum_{k=0}^{n} |f_k^{+}(0)|\,|f_{n-k}^{-}(0)|\right) \\
&+ |\Psi^{+}(0)|\,|\Psi^{-}(0)|\left[\sum_{k=0}^{n} \left(|f_{n-k}^{+\prime}(0)|\,|f_k^{-}(0)| + |f_{n-k}^{-\prime}(0)|\,|f_k^{+}(0)|\right)\right. \\
&\left. + 2\left(\sum_{k=0}^{n-1} |f_{n-k-1}^{+}(0)|\,|f_k^{-}(0)|\right)\right] \\
&\leqslant |A_0|\{2(\tfrac{1}{2}\sigma)^{n-1}\beta + (n-1)(\tfrac{1}{2}\sigma)^{n-2}\beta^2\} \\
&+ (1+2\epsilon)^2\{6(\tfrac{1}{2}\sigma)^{n-1}\beta + 2(2n-3)(\tfrac{1}{2}\sigma)^{n-2}\beta^2\} \equiv g_n.
\end{aligned} \tag{A 23}$$

The radius of convergence of the majorizing series $\Sigma\, k^n g_n$ is determined by the asymptotic behaviour of the g_n:

$$\begin{aligned}
R &= \lim_{n\to\infty} |g_n|^{-1/n} \\
&= \lim_{n\to\infty} |(A_0 + 4(1+2\epsilon)^2)\beta^2 n(\tfrac{1}{2}\sigma)^n|^{-1/n} = 2/\sigma.
\end{aligned} \tag{A 24}$$

Hence, for k satisfying $k < 2/\sigma$, the expression for the dispersion relation converges. This holds only as long as the eigenfunctions are well defined; so once again, since the above bound is larger than k_0, we take $k < k_0$ as the actual domain of convergence.

REFERENCES

Bender, C. M. & Orszag, S. A. 1978 *Advanced Mathematical Methods for Scientists and Engineers.* McGraw Hill.

Davis, R. E. 1969 On the high Reynolds number flow over a wavy boundary. *J. Fluid Mech.* **36**, 337–346.

Drazin, P. G. & Howard, L. N. 1962 The instability to long waves of unbounded parallel inviscid flow. *J. Fluid Mech.* **14**, 257–283.

Drazin, P. G. & Reid, W. H. 1981 *Hydrodynamic Stability.* Cambridge University Press.

Gill, A. E. 1965 A mechanism for instability of plane Couette flow and of Poiseuille flow in a pipe. *J. Fluid Mech.* **21**, 503–511.

Huerre, P. 1980 Nonlinear stability of a free shear layer in the viscous critical layer regime. *Phil. Trans. R. Soc. Lond.* A **293**, 643–675.

Huerre, P. 1983 Finite amplitude evolution of mixing layers in the presence of solid boundaries. *J. Méc.* Special Issue on 2-D Turbulence, p. 121–145.

Huerre, P. 1987 On the Landau constant in mixing layers. *Proc. R. Soc. Lond.* A **409**, 369–381.

Maslowe, S. A. 1981 Shear flow instabilities and transition. In *Hydrodynamic Instabilities and the Transition to Turbulence*, Topics in Applied Physics (ed. H. L. Swinney & J. P. Gollub), vol. 45, p. 181–228. Springer.

MICHALKE, A. 1964 On the inviscid instability of the hyperbolic-tangent velocity profile. *J. Fluid Mech.* **19**, 543–556.

MIKSAD, R. W. 1972 Experiments on the nonlinear stages of free shear layer transition. *J. Fluid Mech.* **56**, 695–719.

ORSZAG, S. A. & KELLS, L. C. 1980 Transition to turbulence in plane Poiseuille flow and plane Couette flow. *J. Fluid Mech.* **96**, 159–205.

SCHADE, H. 1964 Contribution to he nonlinear stability of inviscid shear layers. *Phys. Fluids* **7**, 623–628.

STUART, J. T. 1960 On the nonlinear mechanics of wave disturbances in stable and unstable parallel flows. Part 1. The basic behaviour in plane Poiseuille flow. *J. Fluid Mech.* **9**, 353–370.

STUART, J. T. 1967 On finite amplitude oscillation in laminar mixing layers. *J. Fluid Mech.* **29**, 417–440.

TATSUMI, T. & GOTOH, K. 1960 The stability of free boundary layers between two uniform streams. *J. Fluid Mech.* **7**, 433–441.

TATSUMI, T., GOTOH, K. & AYUKAWA, K. 1964 The stability of a free boundary at large Reynolds numbers. *J. Phys. Soc. Japan* **19**, 1966–1980.

WATSON, J. 1960 On the nonlinear mechanics of wave disturbances in stable and unstable parallel flows. Part 2. The development of a solution for plane Poiseuille flow and plane Couette flow. *J. Fluid Mech.* **9**, 371–389.